Termination and rumpling of nonunique surfaces

P. R. Watson* and J. Mischenko III
Department of Chemistry and Center for Advanced Materials Research, Oregon State University, Gilbert Hall 153, Corvallis, Oregon 97331-4003
(Received 2 February 1990)

Many surfaces in the hcp system can terminate in more than one manner, leading to the nomenclature of a "nonunique surface." We present here the first detailed surface crystallographic examination of this phenomenon, using an R-factor analysis of a large set of low-energy electron diffraction (LEED) data from the clean Ti(10$\bar{1}$0) surface. The data are consistent with a surface covered with domains of both of the terminations that are possible for this surface. Most of the surface, roughly 70%, consists of a termination (B) with a small first interlayer spacing of 0.80 Å. The remainder of the surface terminates in the other possibility (A), where the first interlayer spacing is much larger at 1.80 Å. In the case of the B domains, the measured spacing is contracted relative to the corresponding bulk value of 0.85 Å, whereas the A domains show an expansion of the first interlayer distance compared with the bulk value of 1.70 Å. We suggest that the driving force for this arrangement may be a reduction of rumpling at steps in the surface that separate the domains.

I. INTRODUCTION

The surface crystallography of the hexagonal-close-packed (hcp) metals is much less well developed than that of their cubic counterparts. Furthermore, the few studies that have appeared have concentrated almost exclusively on the basal (0001) surface. These surfaces have proven to have a relatively straightforward crystallography with no indications of complex reconstructions, or even significant deviations from the bulk structure.[1]

An interesting aspect of the crystallography of nonbasal hcp surfaces is the occurrence of "nonunique planes." We can regard such surfaces as being built up from sets of atomic layers that are separated by alternating layer spacings. In some cases the differences in the magnitude of the interlayer spacings can be extreme, being as high as a 5:1 ratio. Even if we assume that the atomic layers terminate at the surface in a bulklike manner, we do not know *a priori* which interlayer spacing will be present at the surface. Thus, unlike the situation for hcp (0001) or the cubic metals, there is a nonuniqueness problem in the surface crystallography of such nonbasal hcp planes. The situation is further complicated by the possibility of the formation of domains of different termination at different points on the surface.

Drawing on our experience from cubic systems, we might further expect that in addition to the possibility of alternate terminations, these nonunique surfaces might well exhibit relaxations of the near-surface interlayer spacings in one or more domains. Indeed, yet further possibilities exist—for instance, reconstructions may occur that bear no relation to the bulk structure.

Previous work in this area is limited to low-energy electron diffraction (LEED) studies of the Co(10$\bar{1}$2) surface by Lambert *et al.*[2] and a study of the Re(10$\bar{1}$0) surface by Zehner and Davis.[3] Both of these investigations assumed a single type of termination to be exclusively present at the surface and led to opposite conclusions concerning the type of termination. One study used only kinematic calculations,[2] which are almost certainly insufficiently accurate, while the second suffered from the use of a very small data set.[3] Hence, while the results of these studies may be indicative, they should be treated with some caution.

We present here the results of a LEED crystallographic study of the Ti(10$\bar{1}$0) surface as a prototype for a nonunique plane system. We have gathered a large amount of experimental data at both normal and off-normal incidence and assessed the degree of fit with calculated $I(V)$ profiles, using several popular R factors. In addition to considering single-domain terminations, we have explored surface structures consisting of regions of both possible terminations, including the possibility of relaxations of the first interlayer spacing.

II. NONUNIQUE PLANE SYSTEMS

Nonunique planes occur when two distinct arrangements of layers of atoms are possible for the same nominal surface plane; such structures do not occur in cubic crystals, but are found for most $\{hkil\}$ planes in the hcp metals. Nonunique planes are those with the four-index notation $\{h,k,-(h+k),l\}$, for which[4]

$$(2h+4k+3l)=6N+\epsilon, \quad N=0,1,2,3,\ldots,$$

where $|\epsilon|=1$, 2, or 3. This type of crystallographic plane, which includes the vast majority of planes in the hcp system, can have two possible arrangements of atoms that are exposed upon formation of a surface by cleavage; the choice of the two arrangements depends upon the position of the cleavage plane within the three-dimensional unit cell. We will here denote the two possible types of surface that result from termination of the bulk structure by A and B, with the convention that the A surface terminates in the larger of the two possible bulk interlayer distances (assuming no relaxation).

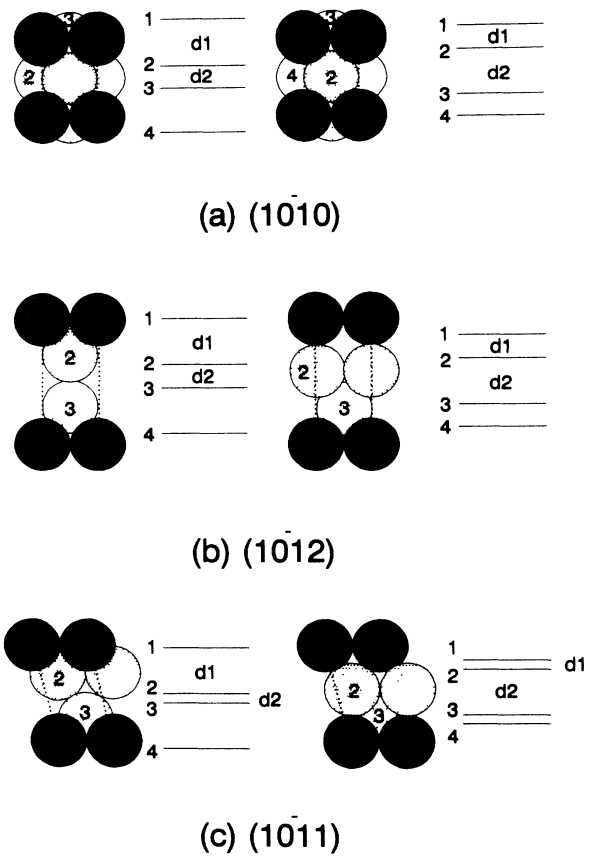

FIG. 1. Schematic diagrams, viewed from above, of some examples of nonunique hcp surfaces and their interlayer spacings for (a) (10$\bar{1}$0), (b) (10$\bar{1}$2), and (c) (10$\bar{1}$1). The depth of shading decreases with distance from the surface into the bulk.

Nonunique plane systems fall into two classes that differ in the degree of disparity between the two possible interlayer distances. This concept is best illustrated with some examples. Figure 1 shows the A and B types of surfaces possible for three nonbasal planes [the difference between A and B surfaces for (0001) is trivial]; some geometrical details are gathered in Table I. For one class, represented by the (10$\bar{1}$0) and (10$\bar{1}$2) planes, we can see that the two arrangements result in layer separations that differ by a factor of 2, the A surface corresponding to $d_1=2d_2$ and the B surface corresponding to $d_2=2d_1$. An example of the second class is provided by the (10$\bar{1}$1) surface, where the A and B arrangements should produce first- and second-layer separations for an ideal surface that are more extreme, differing by a factor of 5.

Real surfaces need not be structurally homogeneous, terminating exclusively in either an A or B arrangement. Domains of different termination can be produced by the occurrence of a step. Mixtures of A and B domains, relaxations, or even a reconstruction that may not be simply related to either the A or B terminations could produce more complex surface crystallographies.

Furthermore, there are qualitative differences in the LEED patterns resulting from step formation between the nonunique and other hcp surfaces, such as (0001). Exclusive A and B terminations of an (0001) surface are indistinguishable, as $d_1=d_2$ for such a surface, except for the orientation of the second layer with respect to the first. For exclusively A or B termination, the threefold symmetry of the surface produces a threefold-symmetric LEED pattern at normal incidence, except that the LEED beams will have switched their intensities between the two symmetrically related sets. The presence of monatomic steps on (0001) will lead to the diffracted intensities adding in proportion to the amount of each domain present, as long as the dimensions of the domains have a larger coherence length, and a smaller physical dimension, than the incident electron beam. Thus, an equal mixture of the two domains should lead to a sixfold-symmetric LEED pattern at normal incidence. Experimentally, hcp (0001) surfaces generally show sixfold-symmetric LEED patterns, confirming the assumption of equal contributions from both domains, although slight variations may occur, e.g., on Zr(0001).[5]

On nonunique hcp surface, on the other hand, the presence of steps is more problematical, even in the absence of relaxations. As d_1 is not equal to d_2 for these surfaces, then exclusive A or B terminations are distinguishable. Thus an A-terminated surface will produce different $I(V)$ curves from a B-terminated surface, not merely a reordering of beam indices. A surface consisting of nonequal amounts of A and B domains will have a complex set of $I(V)$ curves. A nonunique surface containing monoatomic steps can terminate in two crystallographically distinct ways—as A steps on a B surface or vice versa. A step from an A-terminated domain of an hcp(10$\bar{1}$0) surface to a B domain will be shallow, whereas a step from a B domain to an A domain will be high. It may well be that there is a sufficiently high energetic difference between these two processes to produce preferential domain distributions.

III. THE IDEAL Ti(10$\bar{1}$0) SURFACE

In the case of the Ti(10$\bar{1}$0) surface, the bulk structure is built up by repetition of a four-layer sequence involving two different layer spacings that differ by a factor of 2;

TABLE I. Examples of low-index nonunique planes in the hcp system. The index $i=-(h+k)$ in the traditional four-index notation is redundant. Interlayer spacings d_i are in units of a, with $r=(c/a)$.

($hkil$)	N	ϵ	d_1	d_2
10$\bar{1}$0	0	2	$1/\sqrt{3}$	$2/\sqrt{3}$
10$\bar{1}$1	1	-1	$r/2\sqrt{3}(4r^2+3)^{1/2}$	$5r/2\sqrt{3}(4r^2+3)^{1/2}$
10$\bar{1}$2	1	2	$r/2\sqrt{3}(r^2+3)^{1/2}$	$r/\sqrt{3}(r^2+3)^{1/2}$

the relevant bulk interlayer spacings are 1.703 and 0.852 Å. Depending upon which of the two possible interlayer spacings occur at the surface, we can obtain either termination A or B of Fig. 2(a). We choose the A termination to have the larger ideal first interlayer spacing d_1 of 1.703 Å and the B termination the shorter 0.852-Å spacing. We can also see from Fig. 2(a) that the surface has two mirror planes of symmetry in the [10] and [01] directions. As a result, the LEED pattern [Fig. 2(b)] from this surface at privileged incidence directions will show up to fourfold-symmetry relationships between beams. Thus, at normal incidence, the (11) beam is symmetrically related to the $(1\bar{1})$, $(\bar{1}\,\bar{1})$, and $(\bar{1}1)$ beams, whereas (10) is twofold-symmetric with $(\bar{1}0)$. At an off-normal incidence angle that is still contained in one of the mirror planes, e.g., $\phi=90°$, twofold symmetry between beams is still possible, between, for example, the $(1\bar{1})$ and $(\bar{1}\,\bar{1})$ beams.

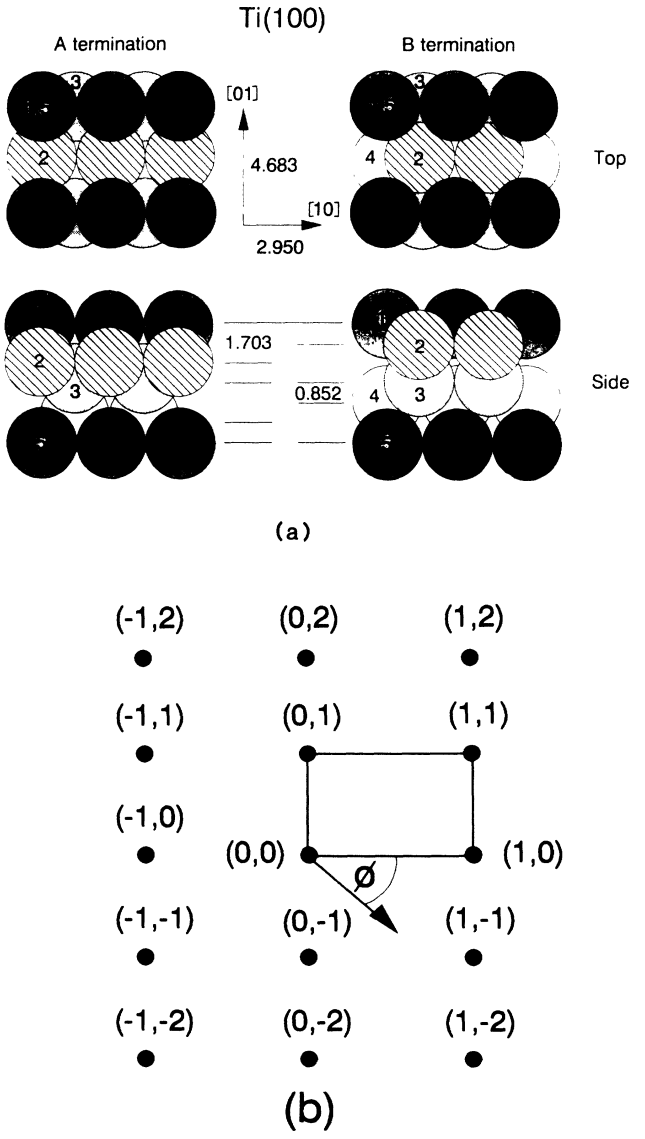

FIG. 2. (a) The structure of the Ti$(10\bar{1}0)$ surface showing two possible terminations resulting from the stacking of layers separated by two interlayer distances that differ by a factor of 2. The numbers indicate different layers starting from the surface. (b) The LEED pattern from a $(10\bar{1}0)$ surface, showing the definition of the azimuthal angle ϕ.

TABLE II. Experimental $I(V)$ data collected from the Ti$(10\bar{1}0)$ surface.

Experimental data set for Ti$(10\bar{1}0)$:			
Temp:	140 K	301 K	
Angle:	$\theta=0°$, $\phi=0°$	$\theta=10°$, $\phi=270°$	
Beams	Range (eV)	Beams	Range (eV)
(01),$(0\bar{1})$	132	(00)	216
(20),$(0\bar{2})$	252	$(0\bar{1})$	216
(03),$(0\bar{3})$	202	(03)	54
(04),$(0\bar{4})$	134	(10),$(\bar{1}0)$	214
(10)	114	$(1\bar{1})$,$(\bar{1}\,\bar{1})$	194
(20),$(\bar{2}0)$	208	(13),$(\bar{1}3)$	46
(11),$(\bar{1}\,\bar{1})$	258	(04)	88
$(\bar{2}\,\bar{2})$	42	$(0\bar{2})$	156
(12),$(1\bar{2})$,	194	(05)	54
$(\bar{1}2)$,$(\bar{1}\,\bar{2})$		(14),$(\bar{1}4)$	82
(13),$(1\bar{3})$,	140	$(1\bar{2})$,$(\bar{1}\,\bar{2})$	128
$(\bar{1}3)$,$(\bar{1}\,\bar{3})$		(20)	116
(21),$(2\bar{1})$,	162	$(2\bar{1})$	78
$(\bar{2}\,\bar{1})$			
	1838		1642

IV. EXPERIMENT

The experiments were performed in a conventional ion-pumped UHV system with a base pressure of about 5×10^{-10} Torr. The Ti single crystal was cut from a boule and polished to maintain a plane within 1° of $(10\bar{1}0)$. Our Ti sample contained sufficient bulk S impurity that surface segregation of S was a persistent problem, and as Ti has a bulk phase change at 880 °C, we were unable to use high-temperature treatments. Hence, cleaning the sample was a lengthy and tedious process. In common with Shih and Jona,[6] we found that cycles of Ar ion bombardment at elevated temperatures of about 650 °C, followed by a short anneal at 600 °C, eventually produced a surface that was clean within the limits of our (RGA) Auger system. This surface appeared to be well-crystallized, as judged by the quality of the LEED pattern. Unlike previous workers,[7] we did not observe any superstructure patterns from this surface *in the absence of surface sulfur.* We have previously concluded[8] that the clean surface does not reconstruct in any manner that disturbs the surface symmetry.

Titanium is a very reactive material, picking up detectable amounts of C and O from the background within one hour of cleaning; hence all LEED experiments were conducted immediately after cleaning and were completed within a few minutes. The LEED $I(V)$ data was taken at 140 K using a 35-mm camera-video system similar to that of Frost *et al.*[9]

We measured a large quantity of data at normal incidence and at $\theta=10°$, $\phi=270°$, the angle being confirmed by analyzing photographs with the method of Cunningham and Weinberg.[10] The total data set included a total

of 24 symmetrically distinct beams covering a total energy range of 3480 eV; further details are provided in Table II. The experimental curves were smoothed and background subtracted, symmetrical beam sets were averaged, and the resulting data normalized to unit beam current.

V. CALCULATIONS

Theoretical $I(V)$ curves were calculated using a modified version of the MO 6.2 routine from the Van Hove–Tong LEED package.[11] The layer-doubling subroutines were changed to allow for the four-layer bulk periodicity of the $(10\bar{1}0)$ system, and for relaxations of d_1. The calculations used the same Ti phase shifts (up to $l=7$) previously used by Lau *et al.*,[12] available in the Van Hove–Tong package. The real part of the inner potential was initially set to -10 eV, though this was later refined during R-factor analysis. Absorption was simulated by an energy-dependent imaginary part[10] of the potential, set by comparison with peak widths in the experiment. The Debye temperature for Ti was taken as 342 K (bulk and surface).

$I(V)$ curves were calculated at 4-eV intervals for both A and B terminations with values of d_1 ranging from 1.5–2.1 Å in 0.1-Å steps for termination A and 0.70–0.95 Å in 0.05-Å steps for the B termination. Calculations ranging from 50 to 270 eV required a few hours of central-processing-unit (CPU) time on a Digital Equipment Corporation VAX11/750 minicomputer. At the smallest interlayer spacing, a persistent instability at about 164 and 188 eV occurred that did not respond to the usual cures, e.g., increasing the iterations allowed in the layer-doubling routine. These pathological points were removed and the curves smoothly joined to the points on either side. Calculated and experimental $I(V)$ curves were compared using the R2,[13] Zanazzi-Jona[14] (RZJ), and Pendry[15] (RPE) R factors.

VI. RESULTS

Due to the large amount of data generated, we have chosen to display only illustrative examples from the complete data set. Figure 3 shows some of the normal-incidence experimental data. We note the good agreement between the symmetrically related (12), $(\bar{1}2)$, $(1\bar{2})$, and $(\bar{1}\,\bar{2})$ beams; similarly, the (02) and $(0\bar{2})$ beams show the expected twofold symmetry (not shown). At off-normal incidence, we also observed the expected symmetries between, e.g., the $(1\bar{1})$ and $(\bar{1}1)$ beams, due to the choice of $\phi=270°$.

In Figs. 4–6 we reproduce some of the comparisons between the experimental data and exclusively A- or B-terminated surface calculations, allowing for different d_1 values. For some beams there appears to be a clear distinction between the fit for an A or B surface. For instance, the (12) beam at normal incidence (Fig. 4), or the $(1\bar{1})$ beam at off-normal incidence (Fig. 5) clearly favor the B-terminated surface. In other cases, the differences in fit between an A and a B type of surface is not very large. The calculated (01) beam $I(V)$ curve at normal incidence (Fig. 6), for instance, gives a similar degree of agreement with experiment for either termination. Both calculations produce peaks in the same regions of the $I(V)$ curve, but with subtle distinctions in peak widths and shapes. It is also apparent that the best agreement for the A calculations occurs at an expanded d_1, relative to the bulk value, whereas, for the B calculations the best agreement seems to be in the opposite direction—that of a contraction from the expected d_1 value.

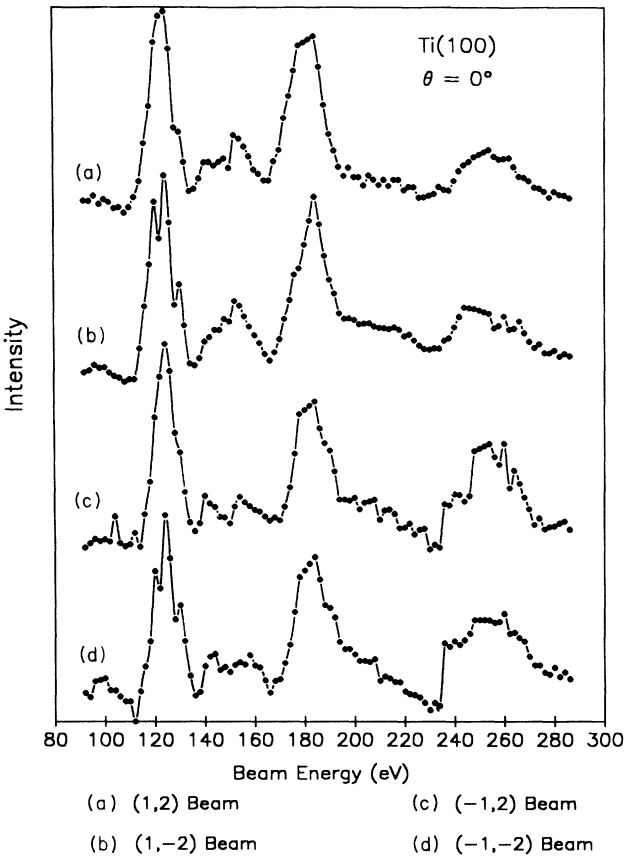

FIG. 3. Experimental $I(V)$ curves measured at normal incidence for symmetrically related beamset (a) (12), (b) $(\bar{1}2)$, (c) $(1\bar{2})$, and (d) $(\bar{1}\bar{2})$.

Clearly, when we are trying to distinguish between two similar surface crystallographies, differentiated by relatively small energies, we need to apply an objective fitting criterion to a large amount of data to be on firm interpretational ground. We therefore summarize, in Table III, the results of R-factor calculations for the above data. The R-factor topographs generally were well defined with clear minima, and a small coupling of d_1 with V_{0r}.

The overall R-factor results for the topmost interlayer spacing are in close agreement between R factors and between data taken at the two different incidence angles. The minimum R-factor values are in the range normally taken as good agreement between theory and experiment. The R factors confirm our visual evaluation in showing a clear preference for the B over the A termination. The best-fit value of d_1 for the B termination, averaged over

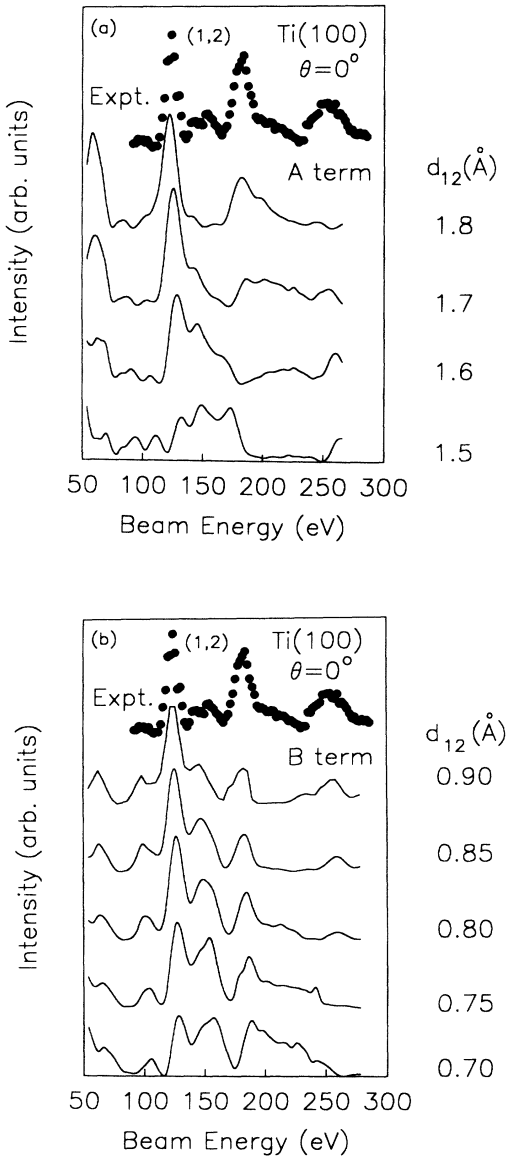

FIG. 4. A comparison of experimental and calculated Ti($10\bar{1}0$) $I(V)$ curves for the (12) beam at normal incidence for (a) an A-terminated surface and (b) a B-terminated surface.

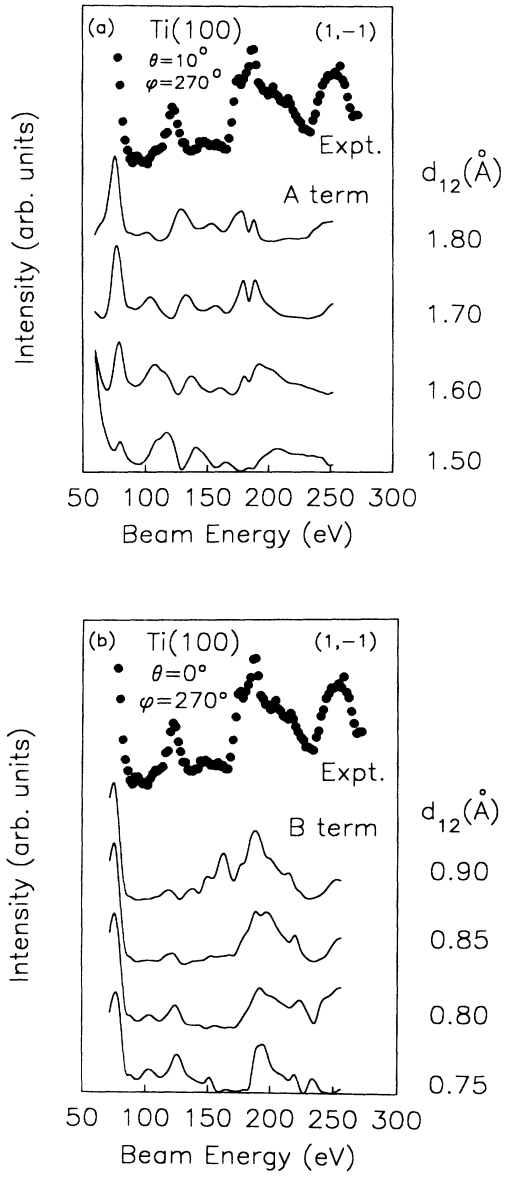

FIG. 5. A comparison of experimental and calculated Ti($10\bar{1}0$) $I(V)$ curves for the ($1\bar{1}$) beam at $\theta=10°$, $\phi=270°$ for (a) an A-terminated surface and (b) a B-terminated surface.

all the data is 0.800 Å for the R2 and RZJ R factors and 0.812 Å for RPE, to better than 0.005 Å, indicating a contraction of 6.1%. We should note that the A-terminated surface, while showing a poorer R factor in all cases, fits best for an averaged value of $d_1=1.734$ Å—equivalent to an *expansion* of 1.8% relative to the bulk value.

There is some scatter in the best-fit values of the inner potential, particularly between the normal and off-normal data. This effect is most probably due to the difference between the work functions of the sample and electron gun filament not being equivalent when the two experiments were conducted (we made no attempt to measure or correct for such effects).

VII. DISCUSSION

Let us first consider the above results in the context of previous work in this area. Only two crystallographic studies of nonunique planes in the hcp system have been reported in the literature; they are for the Co($10\bar{1}2$) (Ref. 2) and Re($10\bar{1}0$) (Ref. 3) surfaces. The authors in these studies did consider the two alternate stacking arrangements of the topmost two surface layers that would produce different terminations, but, unfortunately, both of these studies have defects from the point of view of accurate crystallography. In the case of the Re($10\bar{1}0$) surface studied by Davis and Zehner[3] the data consisted of only two LEED beams and the quoted contraction of 17%

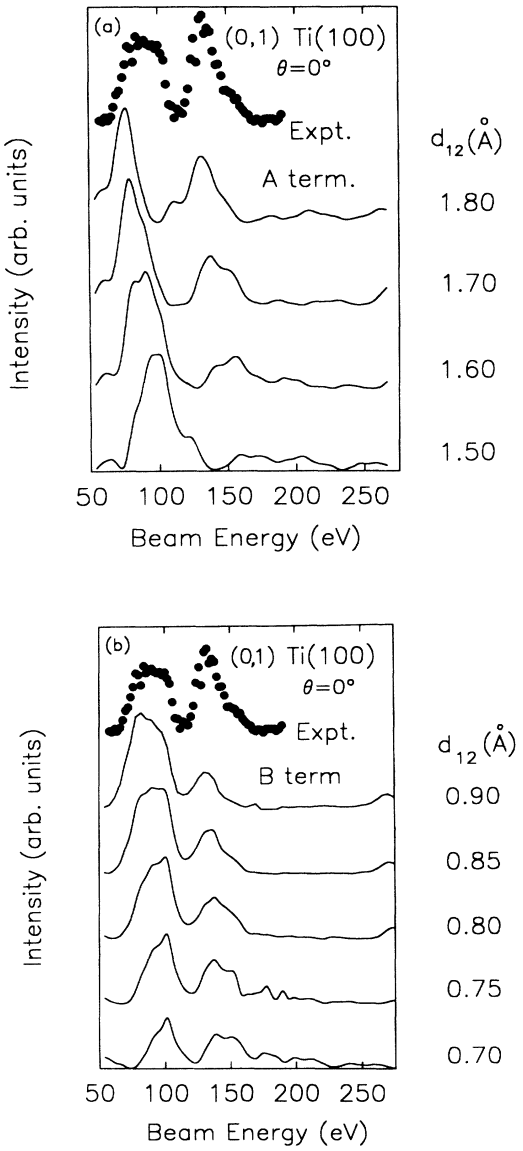

FIG. 6. A comparison of experimental and calculated Ti($10\bar{1}0$) $I(V)$ curves for the (01) beam at normal incidence for (a) an A-terminated surface and (b) a B-terminated surface.

(with a possible multilayer contribution) must be regarded as tentative. Prior *et al.*[2] found the topmost interlayer spacing for Co($10\bar{1}2$) to be within 2% of the bulk value. However, they relied on a kinematical, rather than a full, multiple scattering analysis to distinguish between alternative stacking sequences and hence this result can only be considered as suggestive. Interestingly, the Co($10\bar{1}2$) study favored termination A, with a large d_1, while in the Re($10\bar{1}0$) case the authors came out in favor of termination B, with a small d_1. We should note that this latter paper uses an opposite convention for the sense of terminations A and B from that used here. Both sets of authors state that the surface arrangement they observe is the thermodynamically expected one, but do not give any details of their reasoning.

Our data agree with the results of Zehner and Davis[3] in preferring the B termination (our definition) for a surface exclusively terminated by one domain. Our d_1 value shows a considerably smaller contraction, 6% versus 17%. Part of this difference is more apparent than real, however, as the interlayer separations involved are all small. Thus the 6% contraction we observe for Ti($10\bar{1}0$) is in absolute terms 0.052 Å, while the 17% value of Davis and Zehner for the equivalent Re surface is less than twice this amount at 0.13 Å. However, the much larger data set available in our work prompts us to suggest that the large contraction obtained in the Re($10\bar{1}0$) case may be exaggerated by the small amount of experimental data used.

Our overall best-fit structure, assuming a single termination at the surface, is for the B termination with a first interlayer separation near 0.80 Å. However, the differences in R factors between the A and B terminations shown in Table III, although significant, indicate that the exclusively A termination is still a moderately good fit. Accordingly, we have considered the possibility of an admixture of A and B terminations due to a finite step density within the coherence width of the LEED primary beam. This was done by additively mixing the diffracted intensities from a fraction x of the surface terminated as A with a $(1-x)$ fraction of the B termination and performing new R-factor calculations to search for the values of $d_1(A)$ and $d_1(B)$ in each domain that

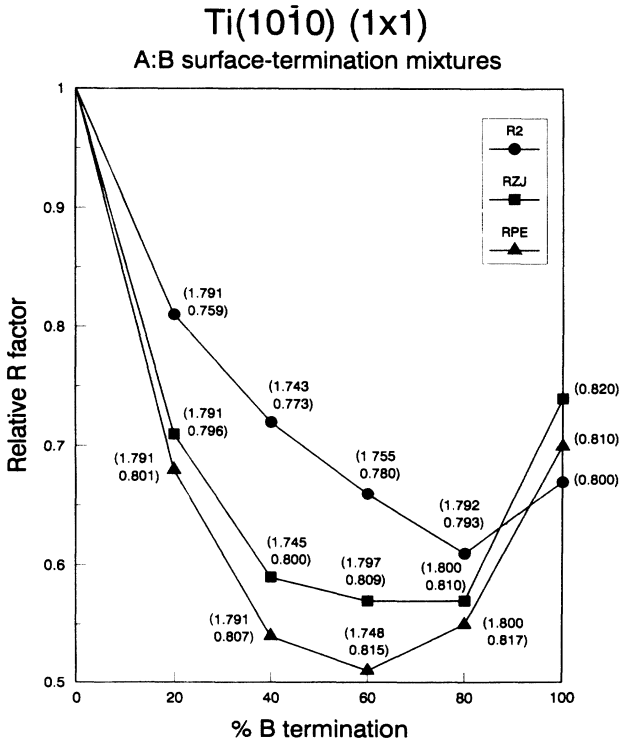

FIG. 7. The effect on the relative value of R factors at the best-fit values of $d_1(A)$ and $d_1(B)$ (shown at each data point) for a Ti($10\bar{1}0$) surface containing various fractions of A and B terminations. Normal-incidence experimental data used with $V_{0r} = -12$ eV.

TABLE III. Summary of R-factor calculations for Ti(10$\bar{1}$0) at $\theta=0°$, and $\theta=10°$, $\phi=270°$, assuming that the surface is uniquely terminated as an A- or B-type surface. R is the global minimum in the R factor, averaged over N experimental beams with an extent of range eV, and occurs at a first interlayer spacing of d_1 and inner potential V_{0r}. The bulk interlayer spacing is 1.703 Å for termination A, and 0.852 Å for termination B.

Angle	Termination	Parameter (minimum value)	R factor R2	RZJ	RPE
$\theta=0°$	A	R	0.1490	0.0849	0.2840
$N=11$		V_{0r} (eV)	10.7	11.8	11.0
Range = 1838		d_1 (Å)	1.728	1.717	1.738
	B	R	0.1052	0.0647	0.1980
		V_{0r} (eV)	13.0	12.1	12.3
		d_1 (Å)	0.800	0.798	0.808
$\theta=10°, \phi=270°$	A	R	0.2425	0.1975	0.3240
$N=13$		V_{0r} (eV)	12.0	14.9	12.1
Range = 1642		d_1 (Å)	1.744	1.740	1.738
	B	R	0.2440	0.1677	0.3186
		V_{0r} (eV)	15.9	14.2	12.9
		d_1 (Å)	0.799	0.801	0.818

simultaneously produce the lowest R factor for the two-domain surface.

Several features of these calculations are noteworthy. We plot in Fig. 7 the variation of the relative R factor (to simplify plotting three different factors) with the fraction of the surface covered in B termination, at the simultaneously best-fit values of $d_1(A)$ and $d_1(B)$ for $V_{0r}=-12$ eV; changes of V_{0r} by ± 2 eV make little difference in the results. There is a clear change, similar for all three factors, in the value of the R factor at the conditions of best fit with experiment as a function of the A:B ratio. This suggests that the composition of the surface is best described as predominantly, but by no means exclusively, B termination. A figure of 60–70 % B termination appears to best describe the data.

The best-fit values of the first interlayer spacing in the B region appear to generally increase by about 0.1 Å as the fraction of the surface covered by B termination is increased from 20% to 80%. At the global minimum $d_1(B)=0.806\pm0.008$Å (-5.4%). The variation in $d_1(A)$ is more chaotic, but a similar trend is apparent. In this case, at the global minimum $d_1(A)=1.80\pm0.01$ Å ($+5.7\%$).

The import of these calculations is that the surface may well be terminated in domains of both A and B terminations, but the basic result seen earlier in the single-termination calculations still holds true—that is, the surface is predominantly B terminated. We would expect that if the system is in thermodynamic equilibrium, then the surface would terminate in a structure with the lower surface tension, i.e., exclusively A or B terminated. The fact that our results suggest that the surface may contain areas of more than one domain may indicate that the surface investigated is not in fact an equilibrium structure. The difficulties alluded to earlier in preparing Ti surfaces without inducing a catastrophic phase change would make preparation of a true equilibrium system difficult.

The other important result from Fig. 7 is that the areas of B termination have a contracted first interlaying spacing, while that in the A-terminated areas is expanded. This curious difference between the A and B regions is worthy of further examination. Consider initially the case where no relaxations are involved and $d_1(A)$ and $d_1(B)$ have their bulk values of 1.703 and 0.852 Å. Our LEED results indicate that the surface is predominantly B terminated. This can be achieved in two ways, as de-

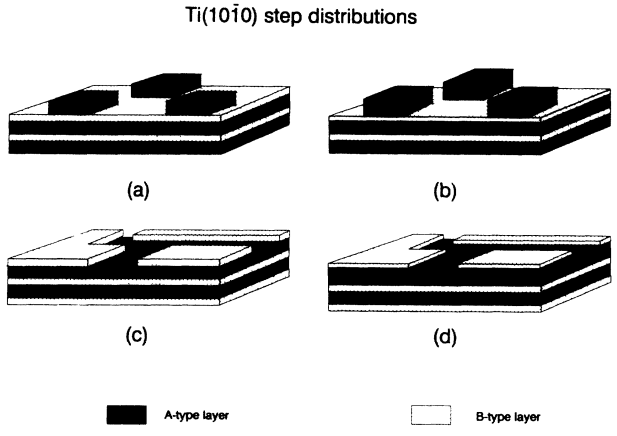

FIG. 8. Schematic diagram of possible step distributions on a Ti(10$\bar{1}$0) surface terminated predominantly by B domains. (a) A domains on a B-terminated surface with no relaxations, (b) A domains on a B-terminated surface with relaxations included, (c) B domains on an A-terminated surface with no relaxations, (d) B domains on an A-terminated surface with relaxations included.

picted in Fig. 8. One is by covering a fraction of a B-terminated surface with A domains, resulting in high steps between the domains [Fig. 8(a)]. The other possibility is to cover most of an A-terminated surface with B domains, resulting in low steps [Fig. 8(c)]. If we now introduce the experimentally determined relaxation effects, we see that contracting $d_1(B)$ and expanding $d_1(A)$ will tend to flatten a low A-to-B step even further [Fig. 8(d)]. On the other hand, the relaxations found here would act in the opposite direction for a B-to-A step—the already high step would increase in height [Fig. 8(b)].

The implication therefore is that it is energetically favorable to minimize the degree of rumpling in a surface by creating low, rather than high, steps. Rather than have a few high A islands on a B surface, we might expect to observe predominantly B domains with shallow holes of A termination separated by low steps, thus minimizing surface rumpling. We cannot assign the source of the energetic benefit of such an arrangement. If a reduction in the height of just the step itself were a prime factor, then we might expect any such influence to decay rapidly away from the step, probably within a few interatomic distances. As the domains are probably of the order of the coherence area of the electron beam—hundreds of angstroms in diameter—the influence of the step would be restricted to the periphery, a small fraction of the total area of the domain. The measured interlayer separations would predominantly reflect those in the interior of the domain. The experimental results indicate that the relaxations of the topmost interlayer spacing, averaged over all the area of a domain, are of opposite sign in the A and B domains. While even larger effects may be operating at the steps themselves, it appears that the source of the relaxations operates over large areas.

VIII. SUMMARY

The analysis of a large amount of normal and off-normal incidence LEED data has led us to the conclusion that the nonunique Ti($10\bar{1}0$) surface is predominantly terminated by a small interlayer spacing domain, although a significant fraction of the surface, perhaps 30%, consists of the other large separation termination. The areas of B termination have a contracted first interlayer spacing (0.800 Å compared with the bulk value of 0.852 Å), while that in the A-terminated areas is expanded relative to the bulk value (1.800 Å compared with 1.703 Å). These results are consistent with a model of the surface where large areas of B termination are separated by shallow holes of A termination, the observed relaxations serving to lower the height of the steps separating the domains, thus minimizing surface rumpling.

There are some assumptions built into our study that may affect the conclusions presented here. One is that the surface atoms remain at their bulk lateral coordinates. We know from our previous work[8] that no lateral movements occur that change the symmetry of the LEED pattern, but we can envisage alterations in atomic coordinates parallel to the surface that would alter the $I(V)$ profiles without changing the overall symmetry. Given the good agreement with the ideal lateral positions used in the calculations here, the likelihood of significant distortions of this type seems small. In any case, LEED analyses of this type are relatively insensitive to these lateral changes. A second assumption is that layers deeper into the bulk than the first may have interlayer spacings that differ from that in the bulk. In all studies to date multilayer relaxations have been strongly damped; hence we feel that it is improbable that changes in deeper layers will affect the essential results of this study.

*To whom correspondence may be addressed.

[1]See, for example, P. R. Watson, J. Phys. Chem. Ref. Data **16**, 953 (1987).
[2]K. A. Prior, K. Schwaha, M. E. Bridge, and R. M. Lambert, Chem. Phys. Lett. **65**, 472 (1979).
[3]H. L. Davis and D. M. Zehner, J. Vac. Sci. Technol. **17**, 190 (1980).
[4]J. F. Nicholas, *An Atlas of Models of Crystal Surfaces* (Gordon and Breach, New York, 1965).
[5]W. T. Moore, P. R. Watson, D. C. Frost, and K. A. R. Mitchell, J. Phys. C **12**, L887 (1979).
[6]H. D. Shih, F. Jona, D. W. Jepsen, and P. M. Marcus, J. Phys. C **9**, 1405 (1976).
[7]A. Khan, Surf. Sci. **48**, 537 (1975).
[8]J. Mischenko III and P. R. Watson, Surf. Sci. **209**, L105 (1989).
[9]D. C. Frost, K. A. R. Mitchell, F. R. Shepherd, and P. R. Watson, J. Vac. Sci. Technol. **13**, 1196 (1976).
[10]S. L. Cunningham and W. H. Weinberg, Rev. Sci. Instrum. **49**, 7 (1978).
[11]M. W. Van Hove and S. Y. Tong, in *Surface Crystallography by LEED,* Vol. 2 of *Springer Series in Chemical Physics* (Springer-Verlag, Berlin, 1979).
[12]B. Lau, B. J. Mrstik, S. Y. Tong, and M. A. Van Hove (unpublished).
[13]M. A. Van Hove, S. Y. Tong, and M. H. Elconin, Surf. Sci. **64**, 85 (1977).
[14]E. Zanazzi and F. Jona, Surf. Sci. **62**, 61 (1977).
[15]J. B. Pendry, J. Phys. C **13**, 937 (1980).

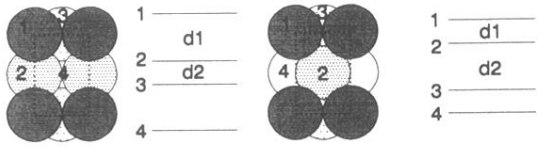

(a) $(10\bar{1}0)$

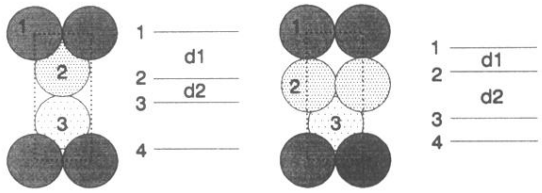

(b) $(10\bar{1}2)$

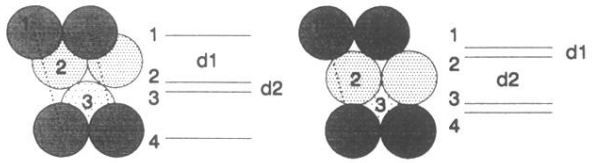

(c) $(10\bar{1}1)$

FIG. 1. Schematic diagrams, viewed from above, of some examples of nonunique hcp surfaces and their interlayer spacings for (a) $(10\bar{1}0)$, (b) $(10\bar{1}2)$, and (c) $(10\bar{1}1)$. The depth of shading decreases with distance from the surface into the bulk.

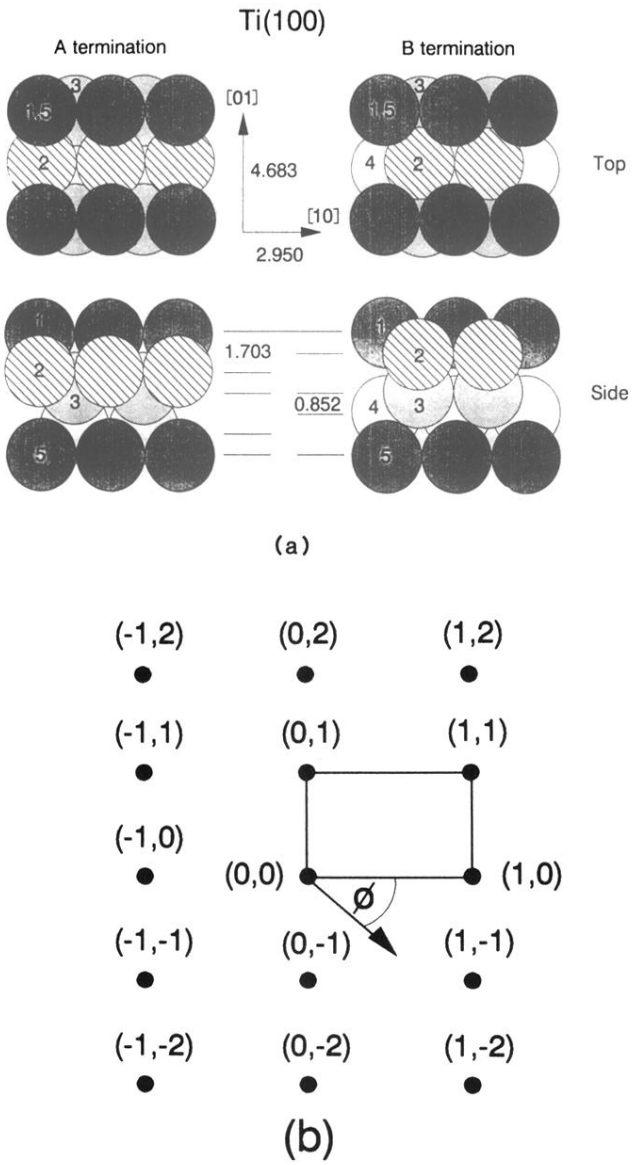

FIG. 2. (a) The structure of the Ti($10\bar{1}0$) surface showing two possible terminations resulting from the stacking of layers separated by two interlayer distances that differ by a factor of 2. The numbers indicate different layers starting from the surface. (b) The LEED pattern from a ($10\bar{1}0$) surface, showing the definition of the azimuthal angle ϕ.

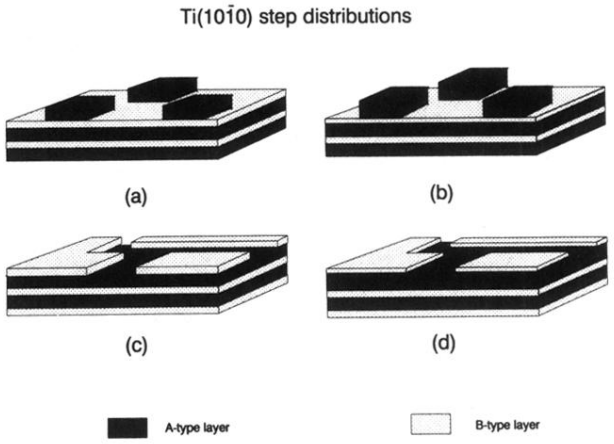

FIG. 8. Schematic diagram of possible step distributions on a Ti($10\bar{1}0$) surface terminated predominantly by B domains. (a) A domains on a B-terminated surface with no relaxations, (b) A domains on a B-terminated surface with relaxations included, (c) B domains on an A-terminated surface with no relaxations, (d) B domains on an A-terminated surface with relaxations included.